Wind and Structures, *Vol. 19, No. 3 (2014) 233-247*
DOI: http://dx.doi.org/10.12989/was.2014.19.3.233

Vortex-induced oscillations of bridges: theoretical linkages between sectional model tests and full bridge responses

Zhitian Zhang[*1], Yaojun Ge[2a] and Zhengqing Chen[3b]

[1]*State Key Laboratory of Disaster Reduction in Civil Engineering, Tongji University, Shanghai, China; Wind Engineering Research Center, Hunan University, Changsha, China*
[2]*State Key Laboratory of Disaster Reduction in Civil Engineering, Tongji University, ShangHai, China*
[3]*Wind Engineering Research Center, Hunan University, Changsha, China*

(Received September 30, 2011, Revised October 26, 2013, Accepted November 8, 2013)

Abstract. Vortex-induced oscillation is a type of aeroelastic phenomenon, to which extended structures such as long-span bridges are most susceptible. The vortex-induced vibration (VIV) behaviors of a concerned bridge were investigated conventionally in virtue of wind tunnel tests on string-mounted sectional models. This necessitates the building of a linkage between the response of the sectional model and that of the prototype structure. Although many released literatures have related to this issue and provided suggestions, there is a lack of consistency among them. In this study, some theoretical models describing the vortex-induced structural motion, including the linear empirical model, the nonlinear empirical model and the modified (or generalized) nonlinear empirical model, are firstly reviewed. Then, the concept of equivalent mass density is introduced based on the principle that an equal input of energy should result in identical structural amplitudes. Based on these, the theoretical linkages between the amplitude of a section model and that corresponding to the prototype bridge are discussed with different analytical models. Theoretical derivation indicates that such connections are dependent mainly on two factors, one is the presupposed shape of deformation, and the other is the theoretical VIV model employed. The theoretical analysis in this study shows that, in comparison to the nonlinear empirical models, the linear one can result in obvious larger estimations of the full bridges' responses, especially in cases of cable-stayed bridges.

Keywords: bridge; vortex shedding; aeroelastic; oscillation; sectional model; full scale

1. Introduction

Vortex-induced oscillation of an elongated structure, such as a long flexible bridge, is one of the most common aeroelastic phenomena due to wind-structure interactions at relative low wind speeds. Most of the bridge deck configurations are aerodynamically bluff, and thus are prone to vortex-induce resonances. The resonance generally occurs when there is a lock-in phenomenon. That means the shedding of vortices in wakes would, over a range of wind speed, match one of the structure's natural frequencies. Many bridges have been reported in the recent decades suffering

*Corresponding author, Associate professor, E-mail: zhangzhitian@hnu.edu.cn
[a] Professor, E-mail: yaojunge@tongji.edu.cn
[b] Professor, E-mail: zqchen@hnu.edu.cn

http://www.techno-press.org/?journal=was&subpage=8 ISSN: 1226-6116 (Print), 1598-6225 (Online)

from perceptible vortex-induced oscillations (Kumarasena 1991, Irwin 2008, Fujino 2002, Larsen 2000, Dale 2006). Further, in some cases, this type of aeroelastic phenomenon has been reported to be even capable of triggering the flutter instability (Matsumoto 2008). Generally, the aeroelastic performances of a bridge concerned are investigated by section model testing in a trial-and-error fashion, allowing for the selection of effective mitigation measures. However, to date, the relation between the response of a sectional model in wind tunnel and that of the corresponding full bridge has not yet been thoroughly understood. Conventionally, we scale up primarily sectional model deflections by the ratio of the full scale length to the sectional model length; then, an additional correction factor accounting for the difference in deformation shape between the rigid sectional model and the full scale bridge is introduced to obtain the maximum response of the full bridge. To date, a variety of “mode shape correction factors” have been suggested to determine the maximum amplitude. Irwin (1998) calculated this correction factor with the assumption of perfectly correlated vortex excitation force to be 1.4. The wind-resistant design manual for highway bridges in Japan suggests it to be $4/\pi$ (Hiroshi 2003), with the assumption of a sinusoidal deformation shape. Based on the linear empirical model, Zhu (2005) determined this factor to be modal-shape dependent and $4/\pi$ in the context of a sinusoidal shape. On the other hand, it will be seen in this study that different theoretical models should result in different “mode shape correction factors”. In view of this and aiming at some analytical models that have been applied rather extensively, theoretical linkages between the VIVs of section models with those of the full scale bridges are discussed.

2. Analytical models

Although much attention has been paid to the turbulence effects to the vortex-induced oscillations (Kawatani 1999, Utsunomiya 2001), this literature discusses only the cases of smooth oncoming flows. There are two general families of analytical models relating to vortex-induced oscillations. The earlier one centers on the so-called wake oscillator model; this kind of models entail the solution of coupled two-degree-of-freedom equations, one describing the body motions and the other describing the wake motions. Various models derived from this generic one were reviewed by Scanlan (1995). Researches have borne out the accuracy of this family of models; but these models need numerous parameters to support them, which generally involve a lot of experiment based identifications and physical reasoning. Therefore, another family of models centered on the single-degree-of-freedom equation of body motion have been developed, typical of which are the linear empirical model (Scanlan 1986), the nonlinear empirical model (Ehsan and Scanlan 1990) and the generalized nonlinear empirical model (Larsen 1995).

According to the linear empirical model, the aerodynamic force per unit length due to the vortex shedding can be expressed as (here take the lift for example)

$$F = \frac{1}{2}\rho U^2 D\left[Y_1(K)\frac{\dot{y}}{U} + Y_2(K)\frac{y}{D} + \frac{1}{2}\tilde{C}_L(t) \right] \tag{1}$$

and

$$\tilde{C}_L(t) = C_L(K)\sin(\omega t + \phi) \tag{2}$$

where Y_1, Y_2, C_L are functions of the reduced frequency $K=D\omega/U$, should be determined experimentally; D is the characteristic size of the body section; U is the velocity of the oncoming flow; ω is the circular oscillation frequency in the case of vortex-induced resonance; y is the vertical motion of the body; ϕ is phase angle.

The vortex-induced resonance occurs usually at a relative low wind speed and the vibrating frequency is generally close to a natural frequency of the structure. Thus, the second term in the square bracket of Eq. (1), namely Y_2, may be negligibly small and the final amplitude of oscillation is dependent on the first and the third term. The main disadvantages of this linear empirical model consist in that it fails to reflect typical properties of vortex-induced oscillations, such as self-exciting and self-limiting. It seems that there are no substantial differences between this model and the harmonic force model being used in early years (Li 1996).

Ehsan and Scanlan (1990) put forward a nonlinear empirical model as

$$F = \frac{1}{2}\rho U^2 D\left[\ Y_1(K)\left(1-\varepsilon\frac{y^2}{D^2}\right)\frac{\dot{y}}{U} + Y_2(K)\frac{y}{D} + \frac{1}{2}\tilde{C}_L(t)\ \right] \tag{3}$$

where the positive constant ε can be determined experimentally. It was shown by Ehsan's work that, in the case of lock-in, $\tilde{C}_L(t)$ in Eq. (3) could be negligibly small. The second term in the square bracket, which represents the aerodynamic stiffness, was also suggested to be negligible (Scanlan 1996). Thus, the vortex-induced lift of Eq. (3) degenerates to

$$F = \frac{1}{2}\rho U^2 D\left[\ Y_1(K)\left(1-\varepsilon\frac{y^2}{D^2}\right)\frac{\dot{y}}{U}\ \right] \tag{4}$$

What actually described by Ea. (4) is a kind of nonlinear damping, depending on both the oscillating velocity and amplitude. The expression exhibits features of a van der Pol oscillator, allowing for negative and positive aerodynamic damping at low and high body displacements, respectively. That means whether the energy is transferred from the flow to the structure or vice versa would be determined by the magnitude of the displacement. Thus, small vibrating amplitudes lead to negative aerodynamic damping and large amplitudes lead to positive damping, corresponding to the self-exciting and self-limiting features of vortex-induced resonance. According to this model, the steady oscillation (limit cycle oscillation) forms when the amplitude reaches the point where the amount of energy transferred from the flow to the structure is just balanced by that dissipated due to mechanical damping.

Larsen (1995) put forward the a generalized nonlinear empirical model, as

$$F = \frac{1}{2}\rho U^2 D\left[\ Y_1(K)\left(1-\varepsilon\left(\frac{y}{D}\right)^{2\nu}\right)\frac{\dot{y}}{U} + Y_2(K)\frac{y}{D} + \frac{1}{2}\tilde{C}_L(t)\ \right] \tag{5}$$

where ν is another parameter which could be obtained experimentally. The generalized nonlinear empirical model owns the same features similar to those of the nonlinear empirical model. Due to the same reason of above mentioned, the second and third term of Eq. (5) can be ignored in the case of lock-in; therefore it can be simplified to

$$F = \frac{1}{2}\rho U^2 D\left[\ Y_1(K)\left(1-\varepsilon\left(\frac{y}{D}\right)^{2\nu}\right)\frac{\dot{y}}{U}\ \right] \tag{6}$$

With the above reviewed analytical models, the linkages between motion amplitudes of a sectional model and the corresponding full bridge are investigated in what follows.

3. Effective mass of the girders

Aerodynamic performances of the long-span bridges are usually investigated in wind tunnel with section models rather than models of the full bridges. Reasons for that include tests on section models being relatively inexpensive, facilitating the investigation of feasible mitigation measures at design stage, etc. Tests on section models afford more flexibilities than on full bridge models, which are generally being used to verify theoretical analyses or section model results. On the other hand, the sectional models can be made at relatively large scales thus allowing for a better modeling of important details and reducing the Reynolds number effects.

In the case of vortex-induced resonance, the bridge structure oscillates generally according approximately to the fundamental modal shapes, vertical or torsional (see Fig. 1). This means that all components such as the main girder, towers, stay cables, etc., are endowed with energy proportional to their corresponding modal deflections. However, only the main girder is supposed to absorb energy from wind during the process of wind-structure interaction. Such an effect (energy accumulated by girder only but allocated and dissipated partially by other components) should be considered when sectional models, instead of full bridge models, are adopted to investigate the aerodynamic performances of prototype structures. The introduction of effective mass would meet this requirement.

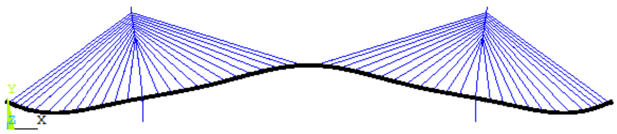

Fig.1 Modal shape of a full bridge

Fig.2. Modal shape of the main girder

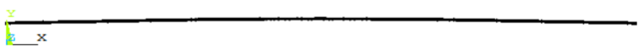

Fig. 3 model of a rigid girder

Fig. 2 shows a suppositional model that comprises the main girder only. It has the same oscillating frequency and modal shape as the girder in the full bridge (Fig. 1). The modal shape shown in Fig. 2 should be viewed as a reduced one of Fig. 1.

If, with an equal energy input, the amplitude of the model in Fig. 2 is expected to be equivalent to that of in Fig. 1, the mass characteristics of the girder shown in Fig. 2 must then be altered and be different from those of the original one in Fig. 1. The calculation of the effective mass is expounded in the follow paragraphs.

Considering the case of lock-in state and supposing the modal shape of the full bridge can be denoted with a vector $\{\varphi\}$, the structural deformation components can be represented in terms of generalized coordinate as

$$\{\varphi\} \cdot q(t) = \{\varphi\} \cdot q_0 \sin(\omega t) \tag{7}$$

where $q(t)$ is the generalized coordinate; q_0 is the amplitude; ω is the structural vibrating frequency, which equals now approximately to a natural frequency.

The velocity vector can be obtained by the first-order derivative of Eq. (7) with respect to time t, as

$$\{\varphi\} \cdot \dot{q}(t) = \{\varphi\} \cdot q_0 \omega \cos(\omega t) \tag{8}$$

Thus, the maximal kinetic energy of the whole structure can be obtained as

$$E_s = \frac{1}{2} q_0^2 \omega^2 \oint_{struc.} m(s) \varphi^2(s) ds \tag{9}$$

where in the oscillating energy of the girder due to the vertical motion is

$$E_b^v = \frac{1}{2} q_0^2 \omega^2 \int_0^L m_v(x) \varphi_v^2(x) dx \tag{10}$$

and that due to torsional motion is

$$E_b^t = \frac{1}{2} q_0^2 \omega^2 \int_0^L m_t(x) \varphi_t^2(x) dx \tag{11}$$

respectively. It is noted that L in Eqs. (10) and (11) is the full length of the main girder, and $m_v(x)$, $m_t(x)$ are the mass and mass moment of inertia per unit length of the main girder, respectively.

The motion magnitude of the suppositional model (Fig. 2) should be equal to that of the full structure (Fig. 1) if the same quantity of energy is inputted. Thus, according to the modal shape function and the original mass density, the effective mass and mass moment of inertia per unit length of the girder at x position can be determined as

$$m_{ev}(x) = m_v(x) \cdot \frac{E_s}{E_b^v} = m_v(x) \cdot \frac{\oint_{struc.} m(s) \varphi^2(s) ds}{\int_0^L m_v(x) \varphi_v^2(x) dx} \tag{12}$$

and

$$m_{et}(x) = m_t(x) \cdot \frac{E_s}{E_b^t} = m_t(x) \cdot \frac{\oint_{struc.} m(s)\varphi^2(s)ds}{\int_0^L m_t(x)\varphi_t^2(x)dx} \tag{13}$$

respectively, where $m_{ev}(x)$ is the effective mass density and $m_{et}(x)$ the effective density of mass moment of inertia.

If a uniform girder and a modal shape function normalized to the mass matrix are involved, Eqs. (12) and (13) can be rewritten as

$$m_{ev} = \frac{1}{\int_0^L \varphi_v^2(x)dx} \tag{14}$$

$$m_{et} = \frac{1}{\int_0^L \varphi_t^2(x)dx} \tag{15}$$

4. Amplitude connections between section model and full bridge

The modal shape shown in Fig. 2 is a suppositional one that represents approximately the actual deformation of the girder in the case of vortex-induced resonance. Such a flexible model is not available for wind tunnel testing; therefore it is replaced generally by a string-mounted rigid section model, as shown in Fig. 3. It is noteworthy that the response of the two-dimensional rigid sectional model in smooth flow is theoretically independent of the model length if only the effects of the edge turbulence are neglected. In view of this, the length of the section model is generally determined according to the size of the wind tunnel available and a proper ratio of width to length. This string-mounted rigid model should own the same frequency, mass, and geometrical characteristics as the flexible one. The only dissimilarity exists in the fact that the string-mounted rigid model has unitary vertical and torsional deflections while the deformations of the flexible model are not unitary. It is this dissimilarity that leads to the employment of mode shape correction factors.

Taking the vertical oscillation for example, the governing equation of motion of the flexible girder model (see Fig. 2) can be written as

$$\ddot{q} + 2\zeta\omega\dot{q} + \omega^2 q = \frac{1}{M_q}\int_0^L \varphi(x)F(x)dx \tag{16}$$

where the modal mass M_q can be expressed, assuming uniformly distributed girder mass, as

$$M_q = \int_0^L \varphi^2(x)m_{ev}(x)dx = m_{ev}\int_0^L \varphi^2(x)dx \tag{17}$$

On the other hand, the governing equation of motion of the string-mounted rigid section model is

$$\ddot{y} + 2\zeta\omega\dot{y} + \omega^2 y = \frac{L}{M_{ev}} F = \frac{F}{m_{ev}} \tag{18}$$

where L is the girder length, ω the circular oscillation frequency, ζ the damping ratio, F the aerodynamic force per unit length due to vortex shedding. The amplitude linkage between a sectional model and a full bridge can be determined by the comparison between the solutions of Eqs. (16) and (18). This will be illustrated in the subsequent sections.

4.1 Linear empirical model

For the flexible model of Fig. 2, the governing equation of motion can be rewritten with the linear empirical model, Eq. (1), and Eq. (16) as

$$\ddot{q} + 2\zeta\omega\dot{q} + \omega^2 q = \frac{1}{2M_q}\rho U^2 D\int_0^L \varphi(x)\left[Y_1\frac{\dot{y}}{U} + Y_2\frac{y}{D} + C\cdot\sin(\omega t+\phi)\right]dx \tag{19}$$

Note in Eq. (19) $y = y(x) = \varphi(x)q$ and $M_q = m_{ev}\int_0^L \varphi^2(x)dx$; thus the following equation can be obtained

$$\ddot{q} + 2\zeta\omega\dot{q} + \omega^2 q = \frac{1}{2m_{ev}}\rho U^2 D\left[Y_1\frac{\dot{q}}{U} + Y_2\frac{q}{D}\right] + \frac{\rho U^2 D\cdot C\cdot\sin(\omega t+\phi)}{2m_{ev}\int_0^L \varphi^2(x)dx}\int_0^L \varphi(x)dx \tag{20}$$

Moving the velocity and displacement related terms in the right side of (20) to the left side results in

$$\ddot{q} + \left(2\zeta\omega - \frac{\rho UDY_1}{2m_{ev}}\right)\dot{q} + \left(\omega^2 - \frac{\rho U^2 Y_2}{2m_{ev}}\right)q = \frac{\rho U^2 D\cdot C\cdot\sin(\omega t+\phi)}{2m_{ev}\int_0^L \varphi^2(x)dx}\int_0^L \varphi(x)dx \tag{21}$$

For the string-mounted rigid model of Fig.3, the governing equation of motion can be written with (1) and (18) as

$$\ddot{y} + 2\zeta\omega\dot{y} + \omega^2 y = \frac{\rho U^2 D}{2m_{ev}}\left[Y_1\frac{\dot{y}}{U} + Y_2\frac{y}{D} + C\cdot\sin(\omega t+\phi)\right] \tag{22}$$

Moving the first and second term in the square bracket of (22) to the left side, one can get

$$\ddot{y} + \left(2\zeta\omega - \frac{\rho UDY_1}{2m_{ev}}\right)\dot{y} + \left(\omega^2 - \frac{\rho U^2 Y_2}{2m_{ev}}\right)y = \frac{\rho U^2 D\cdot C\cdot\sin(\omega t+\phi)}{2m_{ev}} \tag{23}$$

It is noteworthy that Eq. (23) has the same damping and stiffness as those in Eq. (21) except for the loading term in the right side. It is also noted that even though the loading terms share a same sinusoidal form, they differs yet in the amplitudes. Thus, the ratio of the magnitude of modal response of Fig. 2 to that of Fig.3 can be expressed as

$$\frac{q_0}{y_0}=\frac{\int_0^L|\varphi(x)|dx}{\int_0^L\varphi^2(x)dx} \tag{24}$$

where q_0 is the generalized amplitude of the model shown in Fig. 2 and y_0 the amplitude of the model shown in Fig. 3, respectively. The ratio of the maximum response of the model of Fig. 2 to that of the section model of Fig. 3 may then be calculated by

$$\frac{y_{\max}^0}{y_{\max}^1}=\frac{\varphi_{\max}q_0}{y_0}=\frac{\varphi_{\max}(x)\int_0^L|\varphi(x)|dx}{\int_0^L\varphi^2(x)dx} \tag{25}$$

where $y_{\max}^0$ denotes the maximum vertical response of the flexible model of Fig. 2; $y_{\max}^1$ denotes that of the string mounted section model of Fig. 3. Particularly, the ratio will result in a constant of $4/\pi$ in the case of harmonic modal shapes.

4.2 Nonlinear empirical model

If the nonlinear empirical model is employed for the loading of vortex shedding, the governing equation of motion of the girder can be expressed in terms of generalized coordinate of the reduced mode as

$$\ddot{q}+2\zeta\omega\dot{q}+\omega^2q=\frac{\rho U^2D}{2M_q}\int_0^L\varphi(x)\left[Y_1\left(1-\varepsilon\frac{y^2}{D^2}\right)\frac{\dot{y}}{U}\right]dx \tag{26}$$

where $y = y(x) = \varphi(x)q$ and $M_q=m_{ev}\int_0^L\varphi^2(x)dx$.

Substituting M_q into Eq. (26) yields

$$\ddot{q}+2\zeta\omega\dot{q}+\omega^2q=\frac{\rho UD\cdot\dot{q}}{2m_{ev}\int_0^L\varphi^2(x)dx}\int_0^L\varphi^2(x)\left[Y_1\left(1-\varepsilon\frac{\varphi^2(x)\cdot q^2}{D^2}\right)\right]dx \tag{27}$$

Eq. (27) can be rewritten as

$$\ddot{q}+\left\{2\zeta\omega-\frac{\rho UDY_1}{2m_{ev}}+\frac{\rho UY_1\varepsilon q^2}{2m_{ev}D}\cdot\frac{\int_0^L\varphi^4(x)dx}{\int_0^L\varphi^2(x)dx}\right\}\dot{q}+\omega^2q=0 \tag{28}$$

Eq. (28) has the features of the van der Pul oscillator, and its final motion is limit cycle oscillation (LCO), which means the average energy dissipation per cycle is zero. Supposing q=$q_0\sin(\omega t)$ and so that

$$\int_0^{2\pi/\omega}\left\{2\zeta\omega-\frac{\rho UDY_1}{2m_{ev}}+\frac{\rho UY_1\varepsilon q_0^2\sin^2(\omega t)}{2m_{ev}D}\cdot\frac{\int_0^L\varphi^4(x)dx}{\int_0^L\varphi^2(x)dx}\right\}\omega\cos^2(\omega t)dt=0 \tag{29}$$

Eq. (29) yields

$$q_0 = \sqrt{\left(\frac{\rho UDY_1}{2m_{ev}} - 2\zeta\omega\right) \cdot \frac{8m_{ev}D}{\rho UY_1\varepsilon} \cdot \frac{\int_0^L \varphi^2(x)dx}{\int_0^L \varphi^4(x)dx}} \tag{30}$$

It is noteworthy Eq. (30) implies a necessary condition of vortex-induced resonance that the sum of the mechanical damping and the aerodynamic damping should be negative, namely

$$2\zeta\omega - \frac{\rho UDY_1}{2m_{ev}} \leq 0 \tag{31}$$

In the case of string-mounted section model of Fig. 3, the equation of motion is

$$\ddot{y} + 2\zeta\omega\dot{y} + \omega^2 y = \frac{\rho U^2 D}{2m_{ev}} \int_0^L \left[Y_1 \left(1 - \varepsilon \frac{y^2}{D^2}\right) \frac{\dot{y}}{U} \right] dx \tag{32}$$

which can be rewritten as the following quadratic linear homogeneous differential equation

$$\ddot{y} + \left[2\zeta\omega - \frac{\rho UDY_1}{2m_{ev}} + \frac{\rho UY_1\varepsilon y^2}{2m_{ev}D} \right] \dot{y} + \omega^2 y = 0 \tag{33}$$

By the same analytical procedure the steady amplitude can be obtained as

$$y_0 = y_{\max}^1 = \sqrt{\left(\frac{\rho UDY_1}{2m_{ev}} - 2\zeta\omega\right) \cdot \frac{8m_{ev}D}{\rho UY_1\varepsilon}} \tag{34}$$

With Eqs. (30) and (34), the ratio of the maximum response of the model of Fig. 2 to that of the section model of Fig. 3 can be obtained as

$$\frac{y_{\max}^0}{y_{\max}^1} = \frac{q_0 \varphi_{\max}(x)}{y_0} = \varphi_{\max}(x) \sqrt{\frac{\int_0^L \varphi^2(x)dx}{\int_0^L \varphi^4(x)dx}} \tag{35}$$

Furthermore, when the modal shape of the girder $\varphi(x)$ is harmonic (for example sinusoidal), Eq. (35) yields

$$\frac{y_{\max}^0}{y_{\max}^1} = A_0 \sqrt{\frac{\int_0^{n\pi/2} A_0^2 \sin^2 x dx}{\int_0^{n\pi/2} A_0^4 \sin^4 x dx}} = \frac{2\sqrt{3}}{3} \tag{36}$$

It is obvious that this value is less than that derived from the linear empirical model, $4/\pi$, which is suggested by the wind-resistant design manual for highway bridges in Japan (Sato 2003) and also demonstrated by Zhu (2005).

4.3 Generalized nonlinear empirical model

When the generalized nonlinear empirical model is involved, the equation of motion of the model shown by Fig. 2 can be rewritten as

$$\ddot{q}+\left\{ 2\zeta\omega-\frac{\rho UDY_1}{2m_{ev}}+\frac{\rho UDY_1\varepsilon q^{2\nu}}{2m_{ev}D^{2\nu}}\cdot\frac{\int_0^L \varphi^{2(1+\nu)}(x)dx}{\int_0^L \varphi^2(x)dx} \right\}\dot{q}+\omega^2 q=0 \tag{37}$$

In the light of the same procedure as described for the nonlinear empirical model, the average energy dissipation per cycle at LCO state can be expressed, supposing q=$q_0$sin(ωt) , as

$$\int_0^{2\pi/\omega} \left\{ 2\zeta\omega-\frac{\rho UDY_1}{2m_{ev}}+\frac{\rho UDY_1\varepsilon q_0^{2\nu}\sin^{2\nu}(\omega t)}{2m_{ev}D^{2\nu}}\cdot\frac{\int_0^L \varphi^{2(1+\nu)}(x)dx}{\int_0^L \varphi^2(x)dx} \right\}\omega\cos^2(\omega t)dt=0 \tag{38}$$

For string-mounted section model shown in Fig. 3, the equation of motion is

$$\ddot{y}+\left[2\zeta\omega-\frac{\rho UDY_1}{2m_{ev}}+\frac{\rho UDY_1\varepsilon y^{2\nu}}{2m_{ev}D^{2\nu}}\right]\dot{y}+\omega^2 y=0 \tag{39}$$

The average energy dissipation per cycle in the case of (39) is

$$\int_0^{2\pi/\omega} \left\{ 2\zeta\omega-\frac{\rho UDY_1}{2m_{ev}}+\frac{\rho UDY_1\varepsilon y_0^{2\nu}\sin^{2\nu}(\omega t)}{2m_{ev}D^{2\nu}} \right\}\omega\cos^2(\omega t)dt=0 \tag{40}$$

Comparing (38) and (40), one may obtain a necessary condition that make both the two equations hold, as

$$\int_0^{2\pi/\omega} q_0^{2\nu}\frac{\int_0^L \varphi^{2(1+\nu)}(x)dx}{\int_0^L \varphi^2(x)dx}\sin^{2\nu}(\omega t)\omega\cos^2(\omega t)dt=\int_0^{2\pi/\omega} y_0^{2\nu}\sin^{2\nu}(\omega t)\omega\cos^2(\omega t)dt \tag{41}$$

Then, a sufficient condition that makes Eq. (41) hold is

$$\left(\frac{q_0}{y_0}\right)^{2\nu}=\frac{\int_0^L \varphi^2(x)dx}{\int \varphi^{2(1+\nu)}(x)dx} \tag{42}$$

Thus the ratio of the maximum amplitude of the flexible model (Fig. 2) to that of the section model (Fig. 3) can be determined as

$$\frac{y_{\max}^0}{y_{\max}^1}=\varphi_{\max}(x)\left[\frac{\int_0^L \varphi^2(x)dx}{\int_0^L \varphi^{2(1+\nu)}(x)dx}\right]^{\frac{1}{2\nu}} \tag{43}$$

Note that Eq. (43) would converge to the same result as the nonlinear empirical model when the parameter *v* approaching to 1.0.

If the maximum response of a prototype bridge is expected to be evaluated from that tested on a sectional model in wind tunnel, another parameter reflecting the ratio of prototype length to model length should be introduced, and the bearing can be expressed as

$$y_S = \lambda_L \cdot \eta \cdot y_M \tag{44}$$

where y_S is the expected maximum amplitude of the prototype, vertical or torsional, and y_M is that of the section model tested in wind tunnel; λ_L is the ratio of prototype length to model length, η denotes the modal shape factor and

$$\eta = \varphi_{\max}(x) \frac{\int_0^L |\varphi(x)| dx}{\int_0^L \varphi^2(x) dx} \tag{45}$$

when the linear empirical model is adopted, or

$$\eta = \varphi_{\max}(x) \sqrt{\frac{\int_0^L \varphi^2(x) dx}{\int_0^L \varphi^4(x) dx}} \tag{46}$$

when the nonlinear empirical model is adopted, or

$$\eta = \varphi_{\max}(x) \left[\frac{\int_0^L \varphi^2(x) dx}{\int_0^L \varphi^{2(1+\nu)}(x) dx} \right]^{\frac{1}{2\nu}} \tag{47}$$

when the generalized nonlinear empirical model is involved, respectively.

The linkages between the amplitudes of a sectional model and a full-scale bridge due to vortex excitation, in the context of smooth oncoming flow, are summarized in Table 1. It is emphasized that the application of the linkages should be confined to situations of vortex-induced resonances and, moreover, the effects of wind turbulence are not included. It is also worthy of noting that the linkages are dependent apparently on the adopted analytical models and the vibrating shapes of the girder.

5. Numerical examples

Some long-span bridges in China are selected as numerical examples to investigate the above discussed linkages. They are the Qing-lan bridge in Hainan province (cable-stayed bridge, under construction and with a main span of 300 m), the Jin-yue bridge in Hubei province crossing the Changjiang river (cable-stayed bridge under construction, with a main span of 816 m), the Su-tong bridge in Jiangsu province crossing the Changjiang river (cable-stayed bridge, with a main span of 1088 m), the Lie-de bridge in Guangzhou city (self-anchored suspension bridge, with a main span of 219 m), the Ai-zhai bridge in the west of Hunan province (suspension bridge across a deep valley, with a main span of 1176 m) and the Xi-hou-men bridge (suspension bridge, with a main span of 1650 m), respectively.

The η values of a series of typical modes of the above mentioned bridges can be calculated with Eqs. (45), (46) and (47). Table 2 presents the η values as well as the corresponding modal shapes and analytical models. Note that only vertical oscillations are considered.

It can be seen in Table 2 that the linear empirical model, among others, yields the largest modal shape factor mounting up to 1.649 while most of the values derived from the other two are limited to a range from 1.1 to 1.3. It can also be seen from values regarding the generalized nonlinear empirical model that η decreases slightly as the parameter ν increases from 0.25 to 1.5 (η corresponding to ν = 1.0 equals that of the nonlinear empirical model). One may also notice that, for cable-stayed bridges, the factor η is not sensitive to the main span length, especially for the linear empirical model, of which the η keep almost the same value of about 1.6 from span length of 300m up to 1088 m. This value is much larger than the one based on sinusoidal-modal-shape assumption, $4/\pi$. Finally, It can also be noticed in Table 2 that the anti-symmetric mode of the 1176m-span bridge is nearly sinusoidal; therefore it results in the η with the values of 1.275 and 1.16 corresponding to the linear and nonlinear empirical model, which are very close to the theoretical values derived from sinusoidal modal shapes, $4/\pi$ and $2\sqrt{3}/3$, respectively.

Table 1 Conversions of amplitude corresponding to theoretical models

Analytical model	Section model response	Maximum response of full-scale bridge	Maximum response of full-scale bridge (harmonic modal shape)
Linear empirical model	y_M	$\lambda_L y_M \varphi_{\max}(x) \dfrac{\int_0^L \lvert\varphi(x)\rvert dx}{\int_0^L \varphi^2(x)dx}$	$\lambda_L y_M \dfrac{4}{\pi}$
Nonlinear empirical model	y_M	$\lambda_L y_M \varphi_{\max}(x) \sqrt{\dfrac{\int_0^L \varphi^2(x)dx}{\int_0^L \varphi^4(x)dx}}$	$\lambda_L y_M \dfrac{2\sqrt{3}}{3}$
Generalized nonlinear empirical model	y_M	$\lambda_L y_M \varphi_{\max}(x) \left[\dfrac{\int_0^L \varphi^2(x)dx}{\int_0^L \varphi^{2(1+\nu)}(x)dx}\right]^{\frac{1}{2\nu}}$	Dependent upon ν

Table 2 Modal shape factors of some example bridges

Modal shapes of bridges		Main span (m)	η				
			Linear empirical	Nonlinear empirical	Generalized nonlinear empirical model		
					v=0.25	v=0.5	v=1.5
1	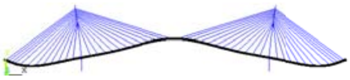	300	1.636	1.288	1.403	1.356	1.241
2	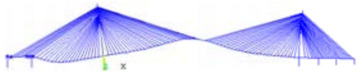	816	1.624	1.248	1.353	1.308	1.209
3	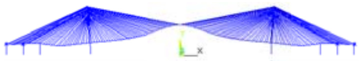	1088	1.649	1.223	1.320	1.277	1.189
4	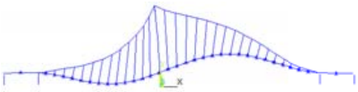	167+219	1.462	1.259	1.329	1.302	1.228
5	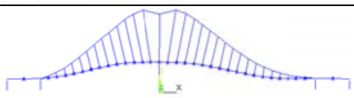	167+219	1.267	1.132	1.169	1.154	1.116
6	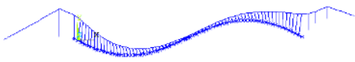	1176	1.275	1.160	1.198	1.183	1.143
7		1176	1.493	1.189	1.267	1.233	1.162
8	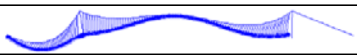	1650	1.411	1.217	1.273	1.250	1.194
9		1650	1.331	1.203	1.246	1.229	1.184

6. Conclusions

Although vortex-induced oscillations are self-limiting in amplitude, the magnitude could be a critical issue concerned by designers. Bridges are judged by many design codes or criteria to be serviceable or not, according to whether the vortex-induced motions exceed a given displacement or acceleration. Such judgments are generally based on experimental studies in wind tunnel with string-mounted sectional models. In contrast with full bridge models, sectional models are generally more reasonable in determining the mitigation measures and in minimizing the influence of Reynolds number. In view of this, it is valuable to investigate linkages between the amplitudes of a sectional model and the expected response of the full scale bridge. Insufficient attention to date has been paid to this issue, and there doesn't see a uniform criterion to describe it. In another aspect, some design codes, such as the current wind-resistant design manual for highway bridges in China, don't provide such a linkage. The research described in this study indicates that such a linkage depends not only on the employed analytical models but also on the deformation shapes. Linkages derived from three different analytical models are discussed and provided. Among them the one derived from the linear empirical model could be rather conservative in comparison to those derived from the nonlinear and the generalized nonlinear empirical models. An investigation of some typical long-span bridges in China as to this type of linkages indicates some interesting characteristics with respect to bridge styles and modal shapes. Finally, it is worthy of mention that what presented in this study cannot provide judgment as to which VIV model is superior to another; however, due to theoretical models could differ in the linkages, future investigations on well-designed sectional and aeroelastic models could in turn result in judgments as to which model is of more physical significance.

Acknowledgments

The work described in this paper was supported by the open project of the state key laboratory of disaster reduction in civil engineering (Project No. SLDRCE10-MB-03), and also supported by the National Science Foundation of China (Project No. 90915002 and 51178182).

References

Dowell, E.H., Clark, R., Cox, D., Curtiss, Jr., H.C., Edwards, J.W., Hall, K.C., Peters, D.A., Scanlan, R., Simiu, E., Sisto, F. and Strganac, T.W. (2004), *A modern course in aeroelasticity*, Fourth revised and enlarged edition, Kluwer academic publishers, New York, USA.

Ehsan, F. and Scanlan, R.H. (1990), "Vortex-induced vibration of flexible bridges", *J. Eng. Mech. - ASCE*, **116**(6), 1392-1411.

Fujino, Y. and Yoshida, Y. (2002), "Wind-induced vibration and control of Trans-Tokyo Bay crossing bridge", *J. Struct. Eng. - ASCE* , **128**(8), 1012-1025.

Hiroshi, S. (2003), "Wind-resistant design manual for highway bridges in Japan", *J. Wind Eng. Ind. Aerod.*, **91**(11), 1499-1509.

Irwin, P.A. (1998), "The role of wind tunnel modelling in the prediction of wind effects on bridges", *Proceedings of the International Symposium Advances in Bridge Aerodynamics*, 10–13 May, Copenhagen. Balkema, Rotterdam.

Irwin, P.A. (2008), "Bluff body aerodynamics in wind engineering", *J. Wind Eng. Ind. Aerod.*, **96**(8), 701-712.

Kawatani M., Toda N., Sato M., Kobayashi H. (1999), "Vortex-induced torsional oscillations of bridge girders with basic sections in turbulent flows", *J. Wind Eng. Ind. Aerod.*, **83**, 327-336.

Kumarasena, T., Scanlan, R.H. and Ehsan, F. (1991), "Wind-induced motions of Deer Isle bridge", *J. Struct. Eng. - ASCE*, **117**(11), 3356-3374.

Larsen, A. (1995), "A generalized model for assessment of vertex-induced vibrations of flexible structures", *J. Wind Eng. Ind. Aerod.*, **57**(2-3), 281-294.

Larsen, A., Esdahl, S., Andresen, J.E. and Vejrum, T. (2000), "Storebaelt suspension bridge -vortex shedding excitation and mitigation by guide vanes", *J. Wind Eng. Ind. Aerod.*, **88**, 283-296.

Li, G.H. (1996), *Stability and vibration of bridge structures*, China railway press, Beijing, China.

Matsumoto, M., Yagi, T., Tamaki, H. and Tsubota, T. (2008), "Vortex-induced vibration and its effect on torsional flutter instability in the case of B/D = 4 rectangular cylinder", *J. Wind Eng. Ind. Aerod*., **96**, 971-983.

Ministry of communications of the People's Republic of China (2004), *Wind-resistant design specification for highway bridges*, People's communications press, Beijing, China.

Simiu, E. and Scanlan, R.H. (1986), *Wind effects on structures: fundamentals and applications to design*, 2nd Ed., John Wiley& Sons Incorporation, New York, USA.

Simiu, E. and Scanlan, R.H. (1996), *Wind effects on structures: fundamentals and applications to design*, 3rd Ed., John Wiley& Sons Incorporation, New York, USA.

Zhu, L.D. (2005), "Mass simulation and amplitude conversion of bridge sectional model test for vortex-excited resonance", *Eng. Mech.*, **22**(5), 204-208. (in Chinese)

CC